

## Configuration and capacitance properties of polypyrrole/aligned carbon nanotubes synthesized by electropolymerization

XU Ying, ZHUANG ShuQi, ZHANG XiaoYan, HE PinGang\* & FANG YuZhi

Department of Chemistry, East China Normal University, Shanghai 200062, China

Received March 1, 2011; accepted May 9, 2011

Aligned carbon nanotubes (ACNTs) were modified with polypyrrole (PPy) *via* electropolymerization. Because of the large specific surface area and excellent electrical conductivity of ACNTs, continuous electropolymerization was able to be carried out, forming a thick PPy coating on the ACNTs. The resulting nanocomposite possessed a core-shell structure with ACNTs as the core, PPy as the shell, and nanoparticles of PPy on the top, and displayed high performance supercapacitance properties.

**aligned carbon nanotubes, polypyrrole, supercapacitance, electropolymerization**

**Citation:** Xu Y, Zhuang S Q, Zhang X Y, et al. Configuration and capacitance properties of polypyrrole/aligned carbon nanotubes synthesized by electropolymerization, Chinese Sci Bull, 2011, 56: 3823–3828, doi: 10.1007/s11434-011-4745-z

Carbon nanotubes (CNTs) were discovered in 1991, and possess many outstanding physical and chemical properties. Since then, this interesting nanomaterial has been developed substantially for science and technology applications. Generally, CNTs are prepared as a randomly oriented structure with each nanotube wrapped with others. Recently, scientists have designed and prepared them with specific structures, such as aligned CNTs (ACNTs) [1], which have been employed as a novel electrode nanomaterial to fabricate bio/chemical sensors [2–4], and electron field emitters [5]. ACNTs are also promising supercapacitor materials because their 3D structure offers a large specific surface area, superior electronic transfer ability through individual nanotubes, and chemical inertness [6–9]. However, because ACNTs are generally directly prepared on substrates without special protection, the nanotubes are easily cracked. In addition, they are intrinsically hydrophobic with a low affinity for aqueous solution. The friability and hydrophobic nature of ACNTs limits their use as supercapacitors. To improve the physicochemical and mechanical properties of ACNTs, and further increase their capacitance, herein, we have modified the nanotubes by electropolymerization with the conducting

polymer polypyrrole (PPy). Conducting polymers such as polyaniline [10], polymethyl methacrylate [11], polythiophene [12] and PPy [13–15] have been combined with traditional CNTs, and such nanocomposite materials display favorable electronic and mechanical properties including enhanced capacitance [16,17].

PPy possesses advantages such as easy synthesis, high electrical conductivity, thermal and chemical stability, environmental friendliness, low preparation cost and electropolymerization potential, in addition to the potential to store energy [18]. However, PPy deposited on common substrates forms an uncontrolled dense film with high resistance to ionic and electronic transfer. The highest reported electronic conductivity of a PPy film is several hundred S/cm [19], which limits its use as an electrode material, supercapacitor, and functional component in microelectromechanical systems. One method to resolve this problem is to use a special matrix with a high surface area and nanoporosity for polymerization of PPy, resulting in a large amount of porous PPy loaded on the matrix surface. CNTs are a good example of such a matrix, and possess the added advantage of increasing the electronic conductivity of PPy. To date, both entangled single- and multi-walled CNTs (*i.e.*, SWCNTs and MWCNTs) have been employed as matrices

\*Corresponding author (email: pghe@chem.ecnu.edu.cn)

for electropolymerization of PPy, improving the specific surface area, electric conductivity and mechanical properties of PPy [20–24]. However, there are few reports on the combination of conducting polymers with ACNTs. Dai and coworkers [25] first reported the electropolymerization of conducting polymers including polyaniline and PPy onto ACNTs for potential application in optoelectronic nanodevices and sensors. The conducting polymers uniformly modified the aligned nanotubes during the electropolymerization process. Windle and coworkers [26] found that electropolymerizing PPy onto ACNTs increased the specific capacitance (SC) by about 4 times compared with a pure PPy film. Wallace et al. [27] fabricated a glucose sensor using a PPy-coated ACNT electrode.

Herein, PPy-ACNT nanocomposites are formed using an electrochemical method. The properties of the nanocomposites are fully investigated, especially the capacitive behavior. Because the ACNTs possess much lower resistance to electron transfer than those with structural defects, individual carbon nanotubes have a high conductivity up to 5000 S/cm, while entangled ones have a conductivity in the order of 200–300 S/cm [28–30]. In addition, the 3D ACNTs possess a much larger surface area than traditional CNTs. Therefore, it was expected that ACNTs would act as a suitable matrix for polymerization of PPy, and the resulting PPy-ACNT nanocomposites would overcome the individual shortcomings of ACNTs and PPy, facilitating their application as supercapacitor materials.

## 1 Experimental

ACNTs were prepared on quartz glass substrate by chemical vapor deposition using iron(II) phthalocyanine as the raw material [31]. They were purified in nitric acid to remove metallic iron particles that were produced during the synthesis of the ACNTs. An Au electrode was then deposited on the ACNTs as a working electrode. The sample was placed in a solution of  $\text{LiClO}_4$  (0.1 mol/L) containing pyrrole (0.2 mol/L). Electropolymerization was carried out using cyclic voltammetry (CV) by scanning between 0 and 1.0 V (vs. Ag/AgCl). After electropolymerization, the resulting PPy-coated ACNTs (ACNTs/PPy) were removed from their original  $\text{SiO}_2$  substrate by treatment in HF solution, and then adhered onto a glassy carbon electrode (GCE,  $\varnothing=4$  mm, geometric surface area is  $12.56 \text{ mm}^2$ ) to form an ACNTs/PPy electrode for electrochemical characterization. A control ACNT electrode was prepared by sputtering a gold layer with a thickness of 200 nm onto a layer of ACNTs, removing the ACNTs from the original  $\text{SiO}_2$  substrate by HF treatment and then adhering the ACNTs onto a GCE ( $\varnothing=4$  mm) [3,32,33].

Electrochemical experiments were performed using an electrochemical workstation (CHI 660A, CH Instruments Co., USA) with a three-electrode system consisting of a

platinum counter electrode, Ag/AgCl (sat. KCl) reference electrode, and ACNT or ACNTs/PPy working electrode. The morphology of the nanocomposites was characterized by scanning electron microscopy (SEM, JEOL-JSM-5610LV, JEOL, Japan) and field emission SEM (FESEM, Hitachi S-4800, Hitachi, Japan). The capacitance of different materials was measured by CV and chronopotentiometry (CP) in KCl solution (1 mol/L). CV experiments were performed at a sweep rate of 100 mV/s, and CP plots were measured under currents of 0.01 and 0.1 mA by controlling the high and low  $E$  limits at 0.8 and 0 V, respectively.

## 2 Results and discussion

### 2.1 Characterization of polypyrrole/aligned carbon nanotube composites

ACNTs were synthesized by chemical vapor deposition under low pressure. The ACNTs possessed a well aligned orientation, as shown in Figure 1(a) and (b). Each CNT was positioned perpendicular to the substrate, herein a  $\text{SiO}_2$  slice, and were uniform both in length (30  $\mu\text{m}$ ) and diameter (100 nm). During the electropolymerization process, individual nanotubes in the ACNTs acted as electronic wires, transferring electrons from the bottom of the electrode to the outmost end of the ACNTs, displaying similar polymerization behavior to that of a GCE modified with entangled MWCNTs [33]. Because of the catalyzing properties of CNTs, the observed oxidation potential of pyrrole was lower than that on GCE (0.65 V), and was similar to that found on a GCE modified with entangled MWCNTs (0.5 V) [34]. Therefore, the polymerization of pyrrole on ACNTs

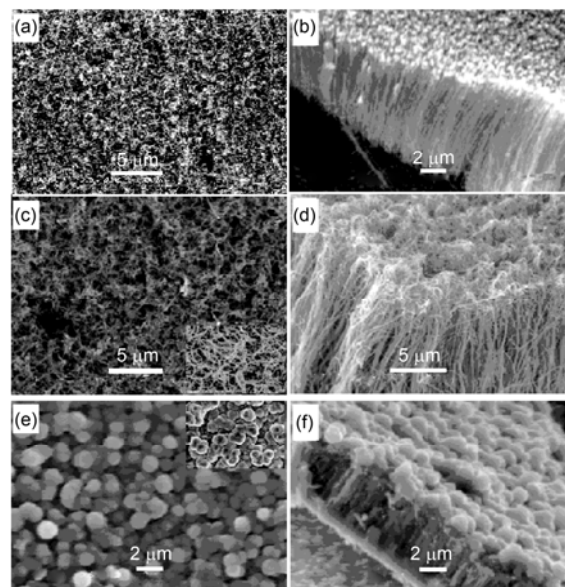


**Figure 1** SEM images showing top and cross-sectional views of (a), (b) ACNTs, and ACNTs/PPy prepared by electropolymerization for (c), (d) 50 cycles, and (e), (f) 100 cycles. The insets in (c) and (e) are FESEM images of the ACNTs/PPy nanocomposites.

can be described as follows: when the potential reached 0.5 V (*vs.* Ag/AgCl), pyrrole monomers surrounding the walls of the ACNTs were oxidized into free radicals. These radicals linked together to form a PPy film, generating a polymer sheath around individual CNTs, *i.e.*, the ACNTs/PPy nanocomposite. The already formed PPy-coated ACNTs would self-catalyze electropolymerization, thus explaining the observed increase in the electropolymerization current during polymerization. The phenomenon of PPy-coated CNTs self-catalyzing PPy electropolymerization was also observed for electropolymerization of PPy onto MWCNTs [34,35]. In addition, because ACNTs provide a large specific surface area for PPy to cover, a large electropolymerization current is generated and the polymerization of PPy onto the ACNT electrode is continuous. In the experiments, the electropolymerization current generated on the ACNT-modified electrode was 17 times that on a bare GCE for the same polymerization cycle [34], and electropolymerization of PPy occurred even after 100 cycles. In contrast, on a traditional GCE electrode, electropolymerization only occurred for around 5 cycles, and then the electropolymerization current stopped increasing [35]. As shown in Figure 1(c) and (d), after electropolymerization the ACNTs were thicker and porous because of the formation of a PPy shell. Importantly, the CNTs maintain their upright orientation. When a traditional substrate is used, it is difficult to control the formation of PPy during electrochemical deposition, and irregular nanoparticles or sediments tend to form [36]. As the number of polymerization cycles was increased, the layer of PPy on the outside of ACNTs thickened until the polymer shells contacted with each other, as shown in Figure 1(e) and (f). Therefore, it could be concluded that the density of the ACNTs controlled the thickness of the PPy shell. Electropolymerization took place not only on the walls of individual nanotubes, but also on their tips to form nanoparticles of PPy, which became much more obvious as the number of electropolymerization cycles increased (Figure 1(e) and (f)). The average diameter of the particles of PPy was estimated to 1  $\mu\text{m}$ . Given that the diameter of each ACNTs/PPy coaxial cylinder was equal to that of the polymer particle at its tip, the radius of the PPy-coated compo-

site was estimated to be 500 nm.

As expected, modification of ACNTs with PPy improved their properties. On one hand, the contact angle of ACNTs/PPy was measured to be  $24.5^\circ$ , which is much smaller than  $146.1^\circ$  for typical hydrophobic ACNTs. The low contact angle of the resulting composite material means that it is hydrophilic, and shows a high affinity for the aqueous phase. On the other hand, decoration with PPy reinforced the structure of the ACNTs, and it was found that the ACNTs/PPy could be removed easily from the  $\text{SiO}_2$  substrate with no obvious destruction of the nanotubes. This facilitated electrode fabrication, and also prolonged the electrode life and improved the reproducibility of results. Without protection from PPy, the uncoated ACNTs cracked and curled easily during removal from the substrate and electrode construction, which limits the use of uncoated ACNTs.

The ACNTs and ACNTs/PPy composites with thin and thick PPy films possessed good electrochemical properties. As shown in the CV plots measured in  $\text{K}_3[\text{Fe}(\text{CN})_6]$  solution (Figure 2), all three electrodes exhibited a reversible redox process with a small peak-to-peak separation and ratio of oxidation to reduction currents equal to 1. In addition, the peak currents were found to be linear versus the square root of the CV sweep rate, *i.e.*,  $v^{1/2}$ , indicating that the redox reaction of  $\text{Fe}(\text{CN})_6^{3-/4-}$  on these electrodes was controlled by diffusion processes. According to the Randles-Sevcik equation, the effective surface area was  $22.1 \times 10^{-2}$ ,  $19.1 \times 10^{-2}$  and  $12.9 \times 10^{-2}$   $\text{cm}^2$  for the bare ACNT electrode, ACNTs/PPy electrode with a thin PPy shell (*i.e.*, 50 electropolymerization cycles) and that with a thick PPy shell (100 electropolymerization cycles), respectively. The smaller electro active area for the ACNTs/PPy electrodes compared with the bare ACNT electrode was mostly caused by the increased electronic resistance of the PPy shell compared with the ACNT core. The capacitance current as shown in the background current in the CV plots (Figure 2), on the other hand, increased continuously with the number of polymerization cycles because the porous PPy film coating the ACNTs offered a larger surface area for ionic transport than the ACNTs.

The electrochemical properties of the electrodes were

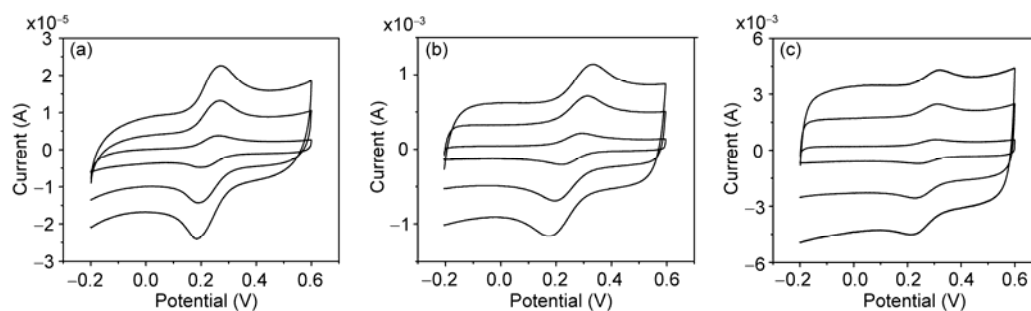


**Figure 2** CVs of  $\text{K}_3[\text{Fe}(\text{CN})_6]$  obtained using (a) the ACNT electrode, and ACNTs/PPy electrodes prepared by electropolymerization for (b) 50 cycles, and (c) 100 cycles with scan rates of 10, 50 and 100 mV/s. The concentration of  $\text{K}_3[\text{Fe}(\text{CN})_6]$  was  $1 \times 10^{-3}$  mol/L for (a) and  $1 \times 10^{-2}$  mol/L for (b) and (c).

evaluated further by electrochemical impedance spectroscopy (EIS). Calculation of the point that intersects with the real axis  $Z_r$  in a Nyquist plot (Figure 3(A)) revealed that the ACNT electrode had the smallest internal resistance  $R_i$  of approximately  $18 \Omega$  (curve a), indicating that the ACNTs possessed excellent electron transfer ability. Modification of the ACNTs with PPy, especially a thick film, increased the resistance to  $24 \Omega$ , which is 30% larger than the bare ACNTs but still low enough to suggest good electronic conductivity.

The increase in electronic resistance after formation of the PPy coating was partially because of the intrinsic lower electronic conductivity of PPy than ACNTs, and the electronic resistance generated at the PPy/ACNT junction when the current flowed between the electrode and the outermost edge of the ACNTs coated with PPy. Observation of the impedance curves in the low frequency region reveals that modification with PPy twisted the impedance line parallel to the imaginary axis  $Z_{im}$ , displaying an ideal shape for an electric double layer capacitor (EDLC) [37]. This was mostly attributed to the porous structure of the PPy network offering an especially large surface to transport electrolyte ions and therefore contributing to the high double layer capacitance of the ACNTs/PPy composite. In contrast, the impedance line for the ACNTs shows a small angle to  $Z_{im}$ , indicating that the ion migration process was slow [38].

## 2.2 Capacitive behavior of polypyrrole/aligned carbon nanotube composites

The capacitive behavior of the ACNTs before and after modification with PPy was investigated by CV within the potential range from 0 to 600 mV (vs. Ag/AgCl). As shown in Figure 3(B), each electrode has a rectangular current-potential curve that has symmetric anodic and cathodic processes, typical of an EDLC [39]. Modification with PPy, especially a thick layer, significantly increased the CV current, which was attributed to the porous PPy film contributing a large double-layer capacitance. The SC of the electrodes were then calculated using the relation  $C=i/(Av)$ , where  $i$  is the average current during the CV scan,  $v$  is the scan rate and  $A$  is the electrode surface area (the geometric surface area of GCE was used, *i.e.*,  $12.56 \text{ mm}^2$ ). The results are compared in Table 1. The ACNTs/PPy composite formed after 100 electropolymerization cycles possessed an SC that was approximately 60 times that of the bare ACNTs. The cycling life of the ACNTs/PPy composite was tested for a large number of voltammetric cycles. The prepared composite exhibited stable electrochemical properties, showing only a 4% decrease in SC after 1000 cycles of CV. Lin and Xu [36] found that SC decreased by 6% for a PPy-MWCNTs composite after 100 cycles of CV. The increased stability of the ACNTs/PPy composite is mostly

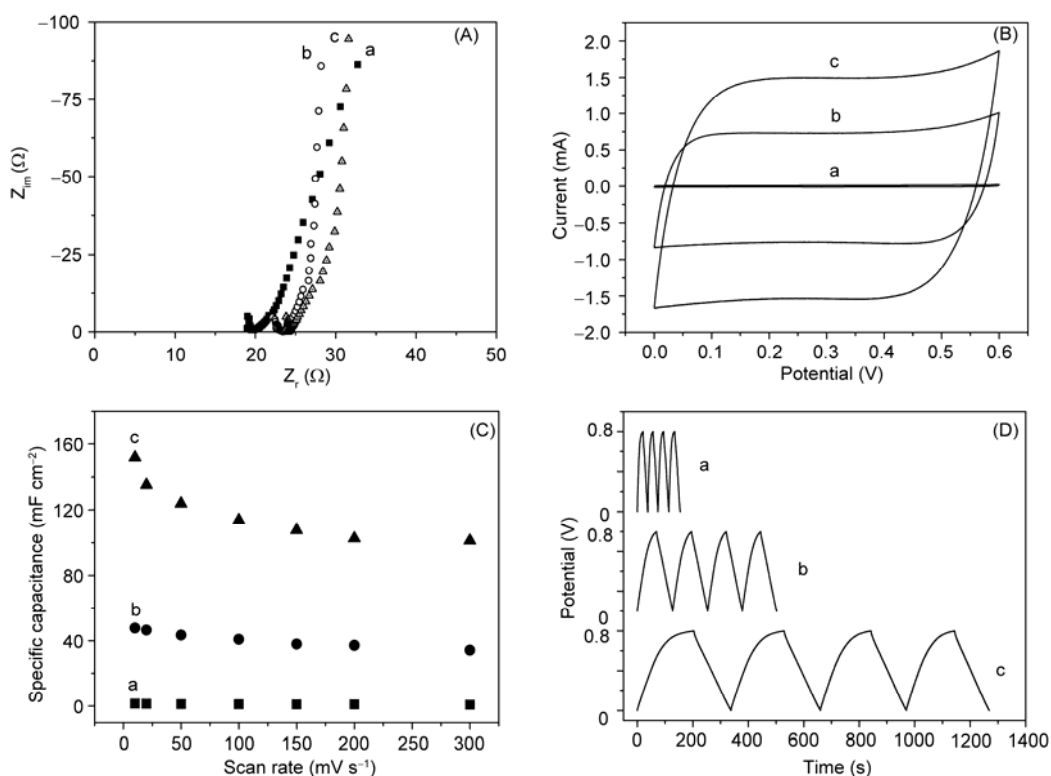


**Figure 3** Electrochemical tests performed using (a) the ACNT electrode, and ACNTs/PPy electrodes prepared by electropolymerization for (b) 50 cycles, and (c) 100 cycles. (A) EIS spectra tested in 1 mol/L KCl solution at open circuit voltage. Figure (B) CV plots obtained in 1 mol/L KCl solution at a scan rate of 100 mV/s. (C) Capacitance vs. scan rate measured by CV. (D) Galvanostatic charge-discharge curves obtained in 1 mol/L KCl solution with a current of (a) 0.01 mA, and (b),(c) 0.1 mA.

**Table 1** SC values of ACNTs and ACNTs/PPy composites formed after different numbers of polymerization cycles

CV (mF/cm <sup>2</sup> )	CP (mF/cm <sup>2</sup> )	Average SC (mF/cm <sup>2</sup> )	Difference in SC (fold)
1.99	1.90	1.95	1
	ACNTs		
	ACNTs/PPy (50 cycles)		
62.18	61.10	61.64	31.7
	ACNTs/PPy (100 cycles)		
116.86	137.12	126.99	65.3

attributed to the very high stability and adherence of the PPy layer formed on the ACNTs by electropolymerization. The SC was determined at various scan rates, and all three electrodes displayed symmetric rectangular CV plots even at a scan rate of 300 mV/s, indicating their quick response and highly efficient charge-discharge processes. Plots of SC as a function of scan rate are shown in Figure 3(C). As the scan rate varied from 5 to 300 mV/s, SC was stable for the bare ACNTs, and decreased from 72 to 52 mF/cm<sup>2</sup> for the ACNTs/PPy with a thin PPy shell. When the PPy film was thick, SC decreased from 155 to 103 mF/cm<sup>2</sup>. This decrease in SC can be attributed to the increased distance for ion diffusion through the thicker polymer film, because at fast scan rates, the ions could not transfer through PPy as quickly as through the bare ACNTs. The resulting dependence of SC of the ACNTs/PPy composites on scan rate was similar to that of a PPy/MWCNTs/GCE composite [36], and much more stable than that of some metal oxides, which showed a 50%–80% decrease in SC at fast scan rates [40]. This indicates that the supercapacitance of the ACNTs/PPy composites is stable.

The charge-discharge behavior of the composites was also examined by CP with multi-cycle scans. As shown in Figure 3(D), the ACNT electrodes with and without PPy modification displayed symmetric charge-discharge curves, indicating reversible charge-discharge reactions with a quick recharge rate, high cyclic efficiency and no obvious charge-discharge memory, which was attributed to the stable electrochemical properties of both PPy and the ACNTs. In addition, the CP plots show that modification with PPy enhances the capacitance by prolonging the charge and discharge times, especially for the ACNTs with a thick PPy layer. The SC was then calculated using the equation  $C=it/(AV)$ , where  $i$  is the applied current,  $t$  is the discharge time,  $A$  is the electrode surface area (12.56 mm<sup>2</sup>), and  $V$  is the voltage limit; the values are presented in Table 1. The values calculated using this method were close to those determined from CV experiments. Averaging these two sets of data revealed that the SC of the thin and thick PPy-coated ACNTs was approximately 30 and 60-fold larger than that of the bare ACNTs, respectively. Thus it can be concluded that the large capacitance of the ACNTs/PPy nanocomposite can be attributed mainly to PPy, with a contribution of

<2% from the ACNT matrix, and a negligible contribution from the GCE. A similar result was obtained using PPy to coat tangled MWCNTs [35]. Therefore, the PPy film was the key factor in the large capacitance of the ACNTs/PPy composite, mostly because of its double layer capacitance. There may also be a minor pseudocapacitance from the electroactivity of PPy, however, this was not obvious during testing. In addition, the increase in SC was precisely controlled by the number of polymerization cycles, which also controlled the amount of PPy deposited, and the thickness of the polymer film on the ACNT matrix. The average diameter of an individual nanotube in the ACNTs is 50–60 nm, and the distance between two nanotubes is 10–20 nm. At the beginning of electropolymerization, the PPy film grows along the ACNT walls, until it becomes thick enough to fill the space between two neighboring nanotubes and link them. After 50 cycles of electropolymerization, the ACNTs/PPy complexes possessed diameters of around 135 nm, which is equal to the distance of two nanotubes and their gap. As electropolymerization progressed, more and more nanotubes were linked with PPy until ACNTs/PPy complexes with a diameter of 1000 nm formed, which includes around 14–17 nanotubes and the gaps between them. However, the increased resistance to electronic and ionic transport in the ACNTs/PPy composite resulted in a minor deviation on the back of the charge curve as shown in Figure 3(D), which became more obvious when the polymer film became thicker.

### 3 Conclusions

The electropolymerization of PPy onto ACNTs was explored. During polymerization, the nanotubes in the ACNTs served as electronic wires, transferring electrons, and catalyzing the oxidation of pyrrole monomers into free radicals, which then combined with each other to construct a polymer shell on the outside of the ACNTs. The resulting ACNTs/PPy nanocomposites maintained their aligned structure and possessed polymer nanoparticles on the tips of the ACNTs. Modification with PPy improved the physicochemical and mechanical properties of the ACNTs, causing them to become hydrophilic, reinforcing their aligned structure, and significantly increasing their capacitance. This was particularly obvious for the ACNTs coated with a thick PPy shell. The ACNTs/PPy composite is a promising supercapacitor material. The tube density of the ACNTs was found to be the key factor determining the amount of PPy electropolymerized, and consequently the increase in SC.

*This work was supported by the National Natural Science Foundation of China (20675031) and "Chen Guang" project supported by Shanghai Municipal Education Commission and Shanghai Education Development Foundation (2008CG30).*

- 1 Li W Z, Xie S S, Qian L X, et al. Large-scale synthesis of aligned carbon nanotubes. *Science*, 1996, 274: 1701–1703
- 2 Zhao K, Zhuang S Q, Chang Z, et al. Amperometric glucose biosensor based on platinum nanoparticles combined aligned carbon nanotubes electrode. *Electroanalysis*, 2007, 19: 1069–1074
- 3 Yang J, Zhang R Y, Xu Y, et al. Direct electrochemistry study of glucose oxidase on Pt nanoparticle-modified aligned carbon nanotubes electrode by the assistance of chitosan-CdS and its biosensing for glucose. *Electrochem Commun*, 2008, 10: 1889–1892
- 4 Gong K, Du F, Xia Z, et al. Nitrogen-doped carbon nanotube arrays with high electrocatalytic activities for oxygen reduction. *Science*, 2009, 323: 760–764
- 5 Jung S M, Jung H Y, Suh J S. Horizontally aligned carbon nanotube field emitters fabricated on ITO glass substrates. *Carbon*, 2008, 46: 1973–1977
- 6 Frackowiak E, Be'guin F. Electrochemical storage of energy in carbon nanotubes and nanostructured carbons. *Carbon*, 2002, 40: 1775–1787
- 7 Du C S, Yeh J, Pan N, et al. High power density supercapacitors using locally aligned carbon nanotube electrodes. *Nanotechnology*, 2005, 16: 350–353
- 8 Lee Y H, An K H, Lee J Y, et al. Carbon nanotube-based supercapacitors. In: Nalwa H, ed. *Encyclopedia of Nanoscience and Nanotechnology*, Vol. 1. Stevenson Ranch: American Scientific Publishers, 2004. 625–634
- 9 Jang J H, Han S, Hyeon T, et al. Electrochemical capacitor performance of hydrous ruthenium oxide/mesoporous carbon composite electrodes. *J Power Source*, 2003, 123: 79–85
- 10 Gupta V, Miura N. High performance electrochemical supercapacitor from electrochemically synthesized nanostructured polyaniline. *Mater Lett*, 2006, 60: 1466–1469
- 11 Sun Y, Wilson S R, Schuster D I. High dissolution and strong light emission of carbon nanotubes in aromatic amine solvents. *J Am Chem Soc*, 2001, 123: 5348–5349
- 12 Panero S, Prosperi E, Klasse B, et al. Characteristics of electrochemically synthesized polymer electrodes in lithium cells: II. Polythiophene. *Electrochim Acta*, 1986, 31: 1597–1600
- 13 Fan L Z, Maier J. High-performance polypyrrole electrode materials for redox supercapacitors. *Electrochem Commun*, 2006, 8: 937–940
- 14 Muthulakshmi B, Kalpana D, Pitchumani S, et al. Electrochemical deposition of polypyrrole for symmetric supercapacitors. *J Power Sources*, 2006, 158: 1533–1537
- 15 Hughes M, Chen G Z, Shaffer M S P, et al. Silylation of multi-walled carbon. *Chem Mater*, 2002, 14: 1610–1633
- 16 Frackowiak E, Jurewicz K, Delpeux S. Nanotubular materials for supercapacitors. *J Power Source*, 2001, 97-8: 822–825
- 17 Downs C, Nugent J, Ajayan P M, et al. Efficient polymerization of aniline at carbon nanotube electrodes. *Adv Mater*, 1999, 11: 1028–1031
- 18 Cui X, Engelhard M H, Lin Y. Preparation, characterization and anion exchange properties of polypyrrole/carbon nanotube nanocomposite. *J Nanosci Nanotechnol*, 2006, 6: 547–553
- 19 Yamaura M, Hagiwara T, Iwata K. Enhancement of electrical conductivity of polypyrrole film by stretching: Counter ion effect. *Synthetic Met*, 1988, 26: 209–224
- 20 Schadler L S, Giannaris S C, Ajayan P M. Load transfer in carbon nanotube epoxy composites. *Appl Phys Lett*, 1998, 73: 3842–3844
- 21 Qian D, Dickey E C, Andrews R, et al. Load transfer and deformation mechanisms in carbon nanotube-polystyrene composites. *Appl Phys Lett*, 2000, 76: 2868–2870
- 22 An K H, Jeon K K, Heo J K, et al. High-capacitance supercapacitor using a nanocomposite electrode of single-walled carbon nanotube and polypyrrole. *J Electrochem Soc*, 2002, 149: A1058–A1062
- 23 Ham H T, Choi Y S, Jeong N, et al. Singlewall carbon nanotubes covered with polypyrrole nanoparticles by the miniemulsion polymerization. *Polymer*, 2005, 46: 6308–6315
- 24 Du C S, Yeh J, Pan N. High power density supercapacitors using locally aligned carbon nanotube electrodes. *Nanotechnology*, 2005, 16: 350–353
- 25 Gao M, Huang S M, Dai L M, et al. Aligned coaxial nanowires of carbon nanotubes sheathed with conducting polymers. *Angew Chem Int Ed*, 2000, 39: 3664–3667
- 26 Hughes M, Shaffer M S P, Renouf A C, et al. Electrochemical capacitance of nanocomposite films formed by coating aligned arrays of carbon nanotubes with polypyrrole. *Adv Mater*, 2002, 14: 382–385
- 27 Gao M, Dai L M, Wallace G G. Biosensors based on aligned carbon nanotubes coated with inherently conducting polymers. *Electroanalysis*, 2003, 15: 1089–1094
- 28 Baughman R H, Chang X C, Zakhidov A A, et al. Carbon nanotube actuators. *Science*, 1999, 284: 1340–1344
- 29 Langer L, Bayot V, Grivei E, et al. Quantum transport in a multi-walled carbon nanotube. *Phys Rev Lett*, 1996, 76: 479–482
- 30 Yap H Y, Ramaker B, Sumant A V, et al. Growth of mechanically fixed and isolated vertically-aligned carbon nanotubes and nanofibers for nanomechanical testing by DC-plasma-enhanced hot filament chemical vapor deposition. *Diam Relat Mater*, 2006, 15: 1622–1628
- 31 Song H Y, Li Y N, Zhao K, et al. Preparation of vertically aligned carbon nanotubes by pyrolysis of phthalocyanine at lower pressure. *Chem J Chin Univ*, 2007, 28: 1622–1627
- 32 Li D C, Dai L, Huang S, et al. Structure and growth of aligned carbon nanotube films by pyrolysis. *Chem Phys Lett*, 2000, 316: 349–355
- 33 Yang J, Xu Y, Zhang R Y, et al. Direct electrochemistry and electrocatalysis of the Hemoglobin immobilized on diazonium-functionalized aligned carbon nanotubes electrode. *Electroanalysis*, 2009, 21: 1672–1677
- 34 Cai H, Xu Y, He P G, et al. Indicator free DNA hybridization detection by impedance measurement based on the DNA-doped conducting polymer film formed on the carbon nanotube modified electrode. *Electroanalysis*, 2003, 15: 1864–1870
- 35 Xu Y, Jiang Y, Cai H, et al. Electrochemical impedance detection of DNA hybridization based on the formation of M-DNA on polypyrrole/carbon nanotube modified electrode. *Anal Chim Acta*, 2004, 516: 19–27
- 36 Lin X Q, Xu Y H. Facile synthesis and electrochemical capacitance of composites of polypyrrole/multi-walled carbon nanotubes. *Electrochim Acta*, 2008, 53: 4990–4997
- 37 Fusalba F, El Mehdi N, Breau L, et al. Physicochemical and electrochemical characterization of polycyclopenta[2,1-b;3,4-b']dithiophene-4-one as an active electrode for electrochemical supercapacitors. *Chem Mater*, 1999, 11: 2743–2753
- 38 Guerrero D J, Ren X, Ferraris J P. Preparation and characterization of poly(3-arylthiophene)s. *Chem Mater*, 1994, 6: 1437–1443
- 39 Conway B E, ed. *Electrochemical Supercapacitors*. New York: Kluwer Academic/Plenum Publishers, 1999
- 40 Prasad K R, Miura N. Potentiodynamically deposited nanostructured manganese dioxide as electrode material for electrochemical redox supercapacitors. *J Power Source*, 2004, 135: 354–360

**Open Access** This article is distributed under the terms of the Creative Commons Attribution License which permits any use, distribution, and reproduction in any medium, provided the original author(s) and source are credited.